Comparative study of microtubule inhibitors – Estramustine and natural podophyllotoxin conjugated PAMAM dendrimer on glioma cell proliferation

ARTICLE *in* EUROPEAN JOURNAL OF MEDICINAL CHEMISTRY · JULY 2013

Impact Factor: 3.45 · DOI: 10.1016/j.ejmech.2013.07.007 · Source: PubMed

3 AUTHORS, INCLUDING:

Ugir Hossain Sk
CSIR - Institute of Himalayan Bioresource T…
34 PUBLICATIONS **395** CITATIONS
SEE PROFILE

Deobrat Dixit
Cleveland Clinic, Lerner Research Institute, …
15 PUBLICATIONS **246** CITATIONS
SEE PROFILE

European Journal of Medicinal Chemistry 68 (2013) 47–57

Contents lists available at ScienceDirect

European Journal of Medicinal Chemistry

journal homepage: http://www.elsevier.com/locate/ejmech

Original article

Comparative study of microtubule inhibitors – Estramustine and natural podophyllotoxin conjugated PAMAM dendrimer on glioma cell proliferation

Ugir Hossain Sk [a,*], Deobrat Dixit [b], Ellora Sen [b]

[a] Natural Plant Products Division, CSIR-Institute of Himalayan Bioresource Technology, Palampur, (H.P.) 176 061, India
[b] National Brain Research Centre, Manesar, Haryana 122051, India

ARTICLE INFO

Article history:
Received 6 April 2013
Received in revised form
15 July 2013
Accepted 18 July 2013
Available online 27 July 2013

Keywords:
Dendrimer-drug conjugation
Estramustine
Podophyllotoxin
Cell cycle
Tubulin depolymerization

ABSTRACT

The synthetic estramustine (EM) and natural podophyllotoxin (PODO) anti-mitotic agents that inhibit tubulin polymerization are known anticancer agents. As low bioavailability limits their anticancer properties, we investigated whether conjugation with PAMAM dendrimer (D) could enhance the activity of D-EM and D-PODO by altering their release pattern. Release kinetics indicated synthesized conjugates to be stable against hydrolytic cleavage and showed sustained release characteristics. However, release of D-EM was slow compared to D-PODO conjugate. Antitumor effect of these conjugates on glioma cells revealed (i) increased cell death and cell cycle arrest (ii) decreased migration and (iii) increased tubulin depolymerization as compared to free drug. Importantly, the effects of natural PODO conjugate on glioma cell survival and migration is more pronounced than D-EM.

1. Introduction

Estramustine (EM) a carbamate ester combining β-estradiol and nornitrogen mustard, one of the most clinically efficient anticancer agent has been used in the treatment of advanced prostatic carcinoma [1]. EM has also been employed in the treatment of astrocytoma, various types of human tumors such as acute myelogenous leukemia, colon, breast and ovary carcinoma either alone or in combination with other anticancer agents [2,3]. EM has shown potent anti-mitotic activity against glioblastoma cells, associated with a rapid disassembly of microtubules [4]. Anti-proliferative effects of EM against malignant glioma both *in-vitro* and *in-vivo* have been reported [5,6]. EM induced cell cycle arrest involves mechanisms that interfere with microtubules, and also acts as inhibitor of microtubules [7,8]. Previous effort to increase the water solubility and bioavailability of EM by converting to EM-phosphate was unable to significantly enhance its biological activity, due to dephosphorylation in *in-vivo* [9]. Other serious side effects induced by EM involves increased risk of venous thrombosis in glioma patients [10].

The natural podophyllotoxins are known for their anti-neoplastic, antitumor and antiviral properties [11,12]. It is effective in the treatment of Wilms tumors, different types of genital tumors and in non-Hodgkin and other lymphomas and lung cancer [13,14]. Combination therapies with PODO are currently being implemented with other chemotherapeutic agents against virus and cancer [11]. PODO in combination with cisplatin is effective in treating neuroblastomas [15]. The mechanism of action of PODO is based on inhibiting tubulin polymerization and arresting cell cycle at the metaphase stage [16,17].

To improve the *in-vivo* stability and aqueous solubility of drugs, several formulations has been considered. Poly(amidoamine) (PAMAM) dendrimers are emerging as prospective candidates for efficient targeted drug and peptide delivery system due to their hyperbranched, well-defined globular nanometer-sized, multiple end modifiable groups and high biocompatibility [18,19]. PAMAM dendrimers are extensively used for diverse biomedical applications and in drug delivery systems [20–23]. In nanomedicine, PAMAM dendrimers have been used for drug delivery platform, by covalently conjugating drug molecules for cancer therapeutics [24–27]. Conjugation of poor-bioavailable drugs with PAMAM dendrimer increases their bioavailability, and decreases dose frequency [20,28]. The covalent attachment of drugs onto dendrimer surfaces offers stable dendrimer–drug conjugates. It is necessary to cleave

* Corresponding author. Tel.: +91 1894 230742x322; fax: +91 1894 230433.
E-mail addresses: ugir@ihbt.res.in, uhocju@gmail.com (U.H. Sk).

0223-5234/$ – see front matter © 2013 Elsevier Masson SAS. All rights reserved.
http://dx.doi.org/10.1016/j.ejmech.2013.07.007

the covalent attachment between drug and dendrimer in order to optimize drug release at the specific biological condition [29]. The covalent linkage of the drugs to the surface functional groups of dendrimer can be achieved via ester or amide or disulphide bond, which can be cleaved hydrolytically or enzymatically or via glutathione [30,31].

There are various reports on the enhancement of the activity of the therapeutic drug upon dendrimer conjugation. The methotrexate (MTX) in conjugation with dendrimer shows 8-fold more toxic effect against resistant human acute lymphoblastoid, as compared to free MTX [25]. Oligonucleotides conjugated PAMAM dendrimer inhibits rat C6 glioma cells *in-vitro* and *in-vivo* [32]. It has also been reported that tamoxifen conjugated to PAMAM dendrimer enhances the blood–brain barrier (BBB) transportation and improves the drug accumulation in glioma cells [33]. The synthesis and application of dendrimer-adriamycin [34] and dendrimer-doxorubicin [35] conjugate for metastasis-associated drug delivery systems has also been reported.

These conjugates may act as classical prodrugs, where enhanced EPR effect increases accumulation into tumor mass, and accelerate crossing the cell membranes via endocytosis to reach their intracellular targets [36,37]. Macromolecule formulated podophyllotoxin-PEG enhances the antitumor activity against solid lung tumor in xenograft model [38]. Recently we have reported the synthesis and enhanced efficacy of dendrimer–cytarabine conjugate against lung epithelial A549 carcinoma cell line [39]. PAMAM dendrimer as drug carriers shows a number of biologically and pharmaco-kinetically desirable properties. However, controlled drug release and high drug loading still remain a challenge. As a result, great attention has been shifted to covalently attaching drugs on the exterior of dendrimers for affording the carriers with higher drug loading capacity and controllable drug release properties.

The aim of this study was to design and synthesize novel PAMAM conjugated estramustine and podophyllotoxin via ester linkage, to improve their pharmacokinetic parameters and release profile kinetics. In this study, we report for the first time the synthesis and extensive characterization of PAMAM dendrimer conjugates with EM and PODO via succinic acid as a linker. To understand the conjugate stability and release kinetics we have monitored comparative control release study *in-vitro* in 0.1 M PBS (pH 7.4), pH 5.4 and DMEM cell culture medium. The cell cytotoxicity assay and cell cycle analysis were performed in human glioma cell lines to access the efficacy of the newly synthesized conjugates.

2. Methods

2.1. Materials

Generation-four hydroxyl-terminated PAMAM dendrimer (D) with ethylenediamine core in methanol solution, benzotriazol-1-yl-oxytripyrrolidinophosphoniumhexafluorophosphate (PyBOP), 4-(dimethylamino)pyridine (DMAP), β-estradiol, tetrabutylammonium bromide (Bu_4NBr), bis(2-chloroethyl)carbamic chloride, succinic anhydride, triethylamine (TEA), diisopropylethylamine (DIEA), trifluoroacetic acid (TFA), dimethylformamide (DMF), DMSO-d_6, $CDCl_3$ were purchased from Sigma–Aldrich Chemical Co. podophyllotoxin (PODO) and anhydrous chloroform ($CHCl_3$) were purchased from Acros Organics. All other solvents and chemicals were purchased from Merck, India and were used without further purification. Snake Skin dialysis Tubing with molecular weight cut-off of 3500 Da was obtained from Thermo Scientific, USA.

All reactions were carried out under nitrogen conditions. Thin-layer chromatography (TLC) was performed on TLC Silica gel 60 F254 plates on aluminum sheets (Merck, Germany), and the spots were visualized with UV (254 nm) light. NMR spectra were recorded on a Bruker Avance-III 600 spectrometer, using commercially available $CDCl_3$ and DMSO-d_6 solvents. Proton chemical shifts are reported in ppm (δ) and tetramethylsilane (TMS) used for internal standard. Coupling constants (J) are reported in hertz (Hz).

2.2. Synthesis of D-EM conjugate

2.2.1. Synthesis of EM (**1**)

To a stirred solution of β-estradiol (0.4 g, 1.4 mmol) in solvent $CHCl_3$–H_2O (5mL/2 mL), Bu_4NBr (0.52 g, 1.62 mmol), NaOH (0.59 g, 14.7 mmol in 2 mL water) were added and the mixture was stirred vigorously for 30 min at room temperature (RT). Then $(ClCH_2CH_2)_2NCOCl$ (0.36 g, 1.76 mmol) in $CHCl_3$ (2 mL) was added drop-wise to the mixture and continuously stirred for another 30 min. TLC indicated absence of starting materials. The resulting mixture was diluted with dichloromethane and the aqueous layer was taken in dichloromethane (2 × 10 mL) and washed with 1 N HCl (2 × 10 mL). The combined organic extracts were washed with brine, dried over anhydrous Na_2SO_4, and concentrated under reduced pressure to deliver crude EM (**1**). The crude product was purified by column chromatography on silica gel (elution with CH_2Cl_2-methanol 98/2) afforded 0.49 g (76% yield) of compound **1**. ^{1}H NMR (600 MHz, $CDCl_3$): δ 7.28 (1H, d, J = 7.2 Hz, Ar–H), 6.88(d, 1H, J = 7.2 Hz, Ar–H), 6.83 (1H, s, Ar–H), 3.84 (2H, s, c-H), 3.75 (6H, s, c and d-H), 2.87 (2H, s, 6-H), 2.33–2.13 (3H, m, 17 and 19-H), 1.97–1.88 (2H, m, 16-H), 1.7–1.19 (9H, m, 7, 9, 11, 12, 14 and 15-H), 0.9 (3H, s, 18-H). ^{13}C NMR (150 MHz, $CDCl_3$): 154.54, 148.59, 138.27, 137.92, 126.38, 121.50, 118.59, 81.87, 51.45, 51.18, 50.09, 44.14, 43.22, 42.00, 41.88, 38.52, 36.69, 30.60, 29.55, 27.05, 26.20, 23.14, 11.05. HRMS (EI) calculated for $C_{23}H_{32}Cl_2NO_3$ [M^++H], 440.1681; found 440.1669.

2.2.2. Synthesis of EM-linker (**2**)

Compound **1** (0.44 g, 1.0 mmol) in dry-$CHCl_3$ (5 mL) was added to a mixture of DMAP (134.2 mg, 1.1 mmol), Et_3N (0.11 g, 1.1 mmol) and succinic anhydride (0.2 g, 2.0 mmol) in anhydrous $CHCl_3$ (5 mL), and the reaction mixture was stirred for 1 h. The resulting mixture was concentrated under reduced pressure to get the crude product. The crude product was purified by column chromatography over silica gel using CH_2Cl_2-methanol 97/3 as eluent. The pure product **2** (530 mg, 98%) was isolated as white solid. ^{1}H NMR (600 MHz, $CDCl_3$): δ 7.27 (1H, d, J = 7.2 Hz, Ar–H), 6.87 (1H, d, J = 7.2 Hz, Ar–H), 6.83 (1H, s, Ar–H), 3.84–3.74 (8H, m, c and d-H), 2.86 (2H, s, 6-H), 2.68–2.66 (4H, d, J = 16.2 Hz, a and b-H), 2.29–2.23 (3H, m, 7 and17-H), 1.88 (2H, d, J = 9.0 Hz, 16-H), 1.74 (1H, s, 9-H), 1.57–1.26 (8H, m, 8, 11, 12, 14 and 15-H), 0.82 (3H, s, 18-H). ^{13}C NMR (150 MHz, $CDCl_3$): 177.5, 172.15, 154.55, 148.6, 138.17, 137.75, 126.41, 121.51, 118.62, 83.16, 51.44, 51.17, 49.78, 43.95, 42.99, 42.0, 38.22, 36.84, 29.51, 29.04, 27.49, 27.01, 26.06, 23.27, 12.05. Mp: 80–81 °C. HRMS (EI) m/z calculated for $C_{27}H_{36}Cl_2NO_6$ [M^++H], 540.1841; found: 540.1833.

2.2.3. Synthesis of D-EM conjugate

The compound **2**(194.7 mg, 0.36 mmol) in dry DMF (3.0 mL) was added to a mixture containing Py-Bop (234.4 mg, 0.451 mmol) and DIEA (70 μL), and the reaction mixture was stirred at RT for 1 h. Then D (320 mg, 0.025 mmol) was added in dry DMF (3 mL) and stirred continuously for 28 h. Again, eight equivalents of Py-Bop and DIEA were added and stirred for another 24 h. The resulting reaction mixture was dialyzed with dialysis membrane (membrane cut-off 3500 Da) for 12 h against DMF solvent. The purified white solid product (450 mg, 94%) was isolated upon evaporation of DMF solvent under vacuum. ^{1}H NMR (600 MHz, DMSO-d_6): δ 8.08–7.71(m, amide–NH from D), 7.26 (1H, Ar–H-1), 6.85 (1H, Ar–H-2),

6.81 (1H, s, Ar–H-4), 4.52 (CH_2 from D), 3.84–3.76 (8H, m, c, d-H from EM), 2.99 (2H, H-6), 2.71–2.78 (m, H-a and b and D-CH_2), 2.4–2.6 (H from D-CH_2), 2.1–2.24 (m, D-CH_2), 1.7–1.73 (m, H-9, H-16 from EM and D-CH_2), 1.34–1.27 (m, H-8, 11, 12, 14, 15 from EM), 0.76 (s, 18-H, from EM).

2.3. Synthesis of D-PODO conjugate

2.3.1. Synthesis of PODO-linker

The succinic anhydride (0.24 g, 2.4 mmol) in anhydrous $CHCl_3$ (2 mL) was added to a mixture of PODO (0.4 g, 0.97 mmol), DMAP (130 mg, 1.06 mmol), Et_3N (0.106 g, 1.06 mmol) in anhydrous $CHCl_3$ (10 mL) at RT and stirred for 1 h. The remaining procedure (purification and isolation) was followed for the synthesis of compounds **2**. The pure white solid product (470 mg, 94%) was isolated. ^{1}H NMR (600 MHz, $CDCl_3$): δ 6.78 (1H, s, 8-H), 6.53 (1H, s, 5-H), 6.38 (2H, s, 13-H), 5.98 (2H, d, J = 8.4 Hz, 2′-H), 5.92 (1H, d, J = 8.4 Hz, 6′-H), 4.59 (1H, s, 11-H), 4.36 (1H, s, 11-H), 4.17 (1H, t, J = 8.4 Hz, 1-H), 3.80 (3H, s, OCH_3), 3.76 (6H, s, 2-O-CH_3), 2.93–2.83 (2H, m, 2 and 3-H), 2.76 (4H, m). ^{13}C NMR (150 MHz, $CDCl_3$): 176.81, 173.79, 172.69, 152.63, 148.17, 147.62, 137.23, 134.85, 132.36, 128.13, 109.73, 108.25, 107.00, 101.61, 73.99, 71.35, 60.76, 56.23, 53.44, 45.54, 43.73, 38.60, 29.04, 28.75. Mp: 104–105 °C. HRMS (EI) m/z calculated for $C_{26}H_{27}O_{11}$ [M^++H], 515.1475; found 515.1482.

2.3.2. Synthesis of D-PODO conjugate

The mixture of compound **3** (0.225 mg, 0.438 mmol), Py-Bop (0.294 mg, 0.567 mmol) and DIEA (100 μL) were suspended in DMF (3.0 mL), and stirred for 1 h at RT in presence of nitrogen. Then the PAMAM dendrimer (D) (366 mg, 0.026 mmol) was added at once in dry DMF (3 mL) and stirred continuously for 24 h. Again eight equivalents of Py-Bop and DIEA were added and stirred for another 24 h. The resulting reaction mixture was dialyzed with dialysis membrane against DMF. Pure white product (500 mg) was isolated on evaporation of volatiles on reduced pressure. ^{1}H NMR (600 MHz, DMSO-d_6): 7.73–8.1 (m, amide –NH from D), 6.89 (s, 1H, Ar–H-8), 6.59 (s, 1H, Ar–H-5), 6.38 (s, 2H, Ar–H-2′ and 6′), 6.01 (m, 2H, H-13), 5.92 (m, 1-H, H-4), 4.56 (CH_2–O from D), 4.27 (m, 1H, H-1), 4.12 (m, 1H, H-11), 3.9 (m, 1H, H-11), 3.61 (s, 3H, -OCH_3 –H), 3.63 (s, 6H, –OCH_3–H), 3.39–2.24 (m, H-2, H-3, and proton from PODO-linker (a and b), and internal D-proton).

2.4. ESI and matrix-assisted laser desorption ionization-time-of-flight mass spectrometry

Electrospray ionization (ESI) mass spectra were recorded on a QTof-Micromass of Waters. Matrix-assisted laser desorption ionization-time of flight (MALDI-TOF) mass spectra were recorded on an AXIMA-CFR Plus spectrometer system equipped with a pulsed nitrogen laser (Shimadzu-Kratos, UK), operating in linear mode and a matrix of 2,5-dihydroxybenzoic acid. Cytochrome *c* (MW 12300 Da) used as external standard. A dendrimer solution was prepared by dissolving 2 mg of dendrimer conjugate (D, D-EM and D-PODO) in 1 mL of ACN: H_20 (1:1). The matrix solution was prepared by dissolving 10 mg of matrix in 500 μL water/ACN (1:1) mixture (containing 0.14% TFA vol/vol). Analytical samples were prepared by mixing 2 μL of dendrimer solution with 20 μL of matrix solution. MALDI-TOF samples were prepared using the over layer method. First, only matrix solution 1 μL was deposited onto a stainless steel sample plate. Following rapid evaporation of solvent, 1 μL of the mixed dendrimer/matrix solution was deposited onto the solid matrix and allowed to dry in air followed by deposition of 1 μL of sample mixture onto a MALDI plate. This mixture was allowed to air dry at RT (22–25 °C).

2.5. High performance liquid chromatography (HPLC) analysis

The conjugates were analyzed in HPLC using Shimadzu Prominence system equipped with LC-20AT quaternary gradient pump, PDA detector (DES-1008D), CBM-20A communication bus module, CTO-10AS vp column oven, SIL-20AC auto-sampler and interfaced with LC solution software (ver.1.21SP1). The HPLC chromatograms were monitored at range 200 nm–300 nm using PDA absorbance detector. All samples and standards were filtered through 0.45 (Millipore) filter. The water/ACN (0.14% w/w TFA) was freshly prepared, filtered, degassed and used as a mobile phase. Symmetry RP-18 reverse phase column with 5 μm particle size, 25 cm length, 4.6 mm internal diameter was used. A gradient flow was used with initial condition 50:50 to 5:95 (H_2O/ACN) in 40 min and returning to 50:50 (H_2O/ACN) in 60 min with flow rate of 1 mL/min for D-EM conjugate. A gradient flow was used with initial condition 90: 10 to 50:50 (H_2O/ACN) in 30 min and returning to 90:10 (H_2O/ACN) in 55 min with flow rate of 1 mL/min for D-PODO conjugate. The non-complexes EM, EM-linker, PODO, PODO-linker, and MDPODO were analyzed by calibration curve.

2.6. Drug release study of the conjugates in PBS (pH 7.4), DMEM cell culture medium and acidic pH

Release of drug EM and PODO from conjugates were characterized in PBS (pH 7.4) at 37 °C. D-EM (2 mg/mL) and D-PODO (2 mg/mL) were incubated in 0.1 M PBS with constant shaking in water bath, a mixture (500 μL) was withdrawn at periodic intervals and ACN (500 μL) was added to make the final concentration 1 mg/mL. The solution was then filtered through 0.45 μm filter and stored at −20 °C until HPLC analyses. The samples were analyzed by HPLC to evaluate the stability of the conjugates and release of EM and PODO, from their corresponding conjugates (D-EM and D-PODO). Release drug concentrations were measured from their respective standard graph (Fig. S1).

Similarly, conjugates were incubated at 37 °C in DMEM cell culture medium containing 10% FBS and 1.0% antibiotics. The concentration of the conjugates 2 mg/mL was maintained throughout the experimental period. The 500 μL medium mixture were withdrawn and diluted with ACN to make the final concentration 1 mg/mL and analyzed in HPLC by following the same methodology applied for release study in PBS. The release study of the conjugates in (pH 5.4) is also monitored by following above mention methodology.

2.7. Determination of hydrodynamic diameter and zeta potential

The particle size and zeta potential of D, D-EM and D-PODO were determined by dynamic light scattering (DLS) using a Zetasizer Nano ZS (Malvern Instrument Ltd., MAL1049758, Worchester, U.K) equipped with a 50 mWHe-Ne laser (633 nm). The conjugates (D-EM and D-PODO) and starting D were dissolved in HPLC water to make the solution with the final concentration of 0.5 mg/mL. The solution was filtered through a Millipore filter (0.45 micron, Millex-HN) and DLS measurements were performed at 25 °C with a scattering detector angle of 173° in triplicate.

2.8. Transmission electron microscope (TEM)

The particle images were carried out in TEM (JEOL) to study particles morphology. The D-EM and D-PODO conjugates were dispersed in ACN and a drop of dispersed particle was placed on Cu-grid for determining the shape and size.

2.9. Cell culture and treatment

Glioblastoma cell lines A172, U87MG and T98G were obtained from American Type Culture Collection (ATCC, Manassas, VA USA)

and cultured in DMEM supplemented with 10% fetal bovine serum. On attaining semi-confluence, cells were switched to serum free media (SFM) and after 12 h, cells were treated with different concentrations of EM, D-EM, PODO and D-PODO (in dimethyl sulphoxide, DMSO) in SFM for 24–48 h. DMSO treated cells were used as controls. All reagents were purchased from Sigma (St. Louis, MO) unless otherwise stated.

2.10. Determination of cell viability

Viability of glioma cells treated with EM, PODO, D-EM and D-PODO, for 48 h in 96-well plates were assessed using the MTS assay (Promega) as described [40]. Values are expressed as percentage change compared to controls.

2.11. Cell cycle analysis

To determine the effect of EM, PODO, D-EM and D-PODO on cell cycle progression, FACS analysis of DNA contents were performed as described [41] using Cell Quest program on FACS Calibur (Becton Dickinson, CA, USA). The percentages of cells in the G1, S, and G2/M phases of the cell cycle were analyzed with the Cell Quest pro software as described [41].

2.12. Determination of tubulin polymerization

Following treatment with EM, PODO, D-PODO and D-EM for 24 h, glioma cells were suspended in 100 mM HEPES buffer containing 2 mM GTP and homogenized thoroughly. Cell homogenate was centrifuged to pellet cell organelles and supernatant was again centrifuged at 100,000× g for 1 h to separate polymerized fraction in pellet and globular fraction in supernatant. Western blot analysis was performed to detect tubulin in different fractions.

2.13. Wound-healing assay

To determine the effect of EM, PODO, D-EM and D-PODO on glioma cell migration wound healing assay was performed as described previously [42]. Briefly, upon reaching semi-confluence cells were grown in serum free media for 12 h and a plastic pipette tip was drawn across the center of the culture to produce a clean wound area. Cells were then left untreated or treated with EM, PODO, D-PODO and D-EM for 24 h and cell movement in the wound area was examined. The migration distance between the leading edge of the migrating cells and the edge of the wound at the end of treatment was taken by light microscopy as described [42].

3. Results

3.1. Synthesis of dendrimer-estramustine (D-EM) and dendrimer-podophyllotoxin (D-PODO) conjugates

The drugs EM and PODO possess secondary hydroxyl reactive group. Herein, we have used succinic acid as a linker to conjugate EM and PODO to the dendrimer surface. The synthetic route of the dendrimer conjugates (D-EM and D-PODO) is depicted in Fig. 1a

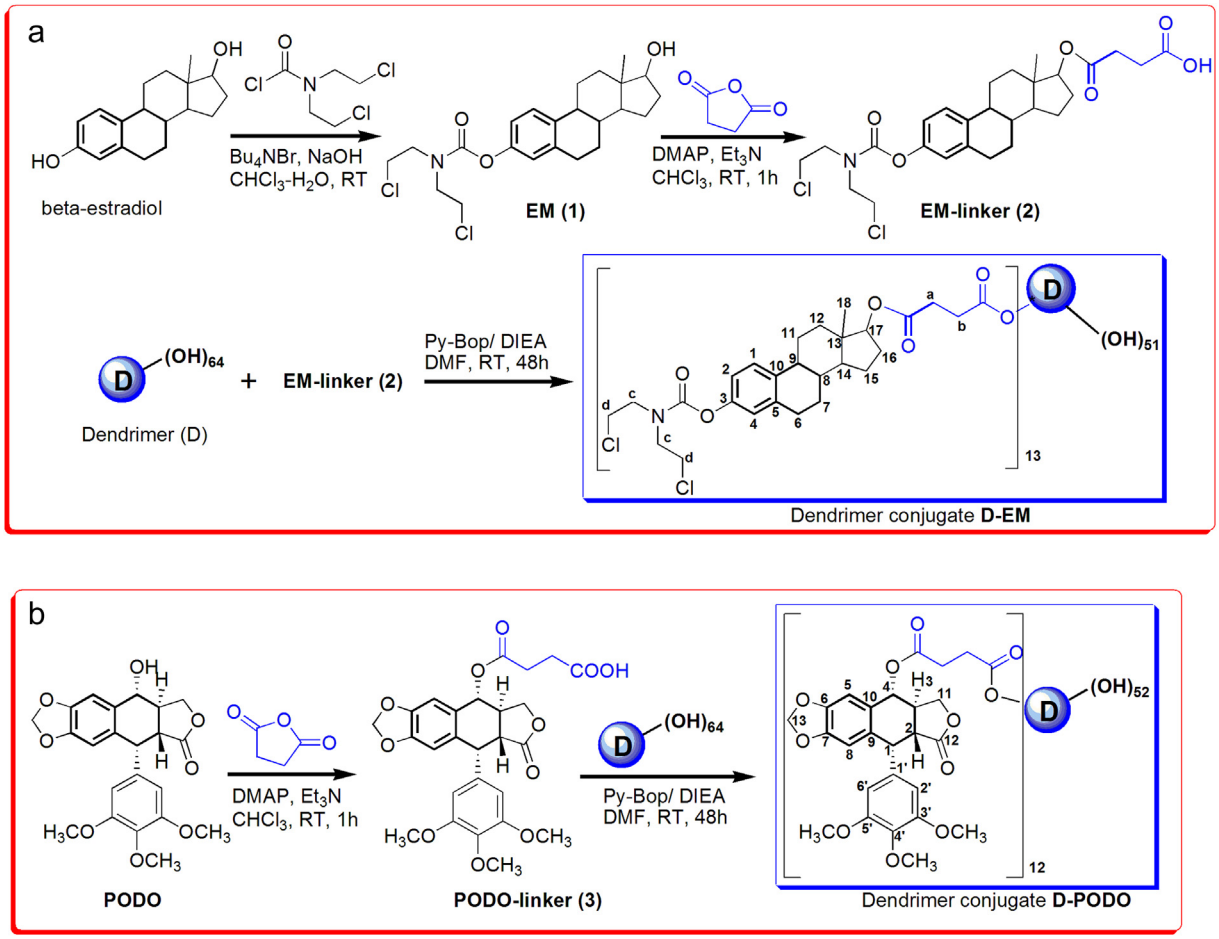

Fig. 1. (a). The synthesis of estramustine-dendrimer (D-EM) conjugate using succinic acid as linker. (b). Synthesis of podophyllotoxin-dendrimer (D-PODO) conjugate using succinic acid as linker.

and b. The attachment of the mustard moiety to the β-estradiol was successfully achieved by reacting with commercially available *N,N*-bis(2-chloroethyl)-carbamoyl chloride in presence of Bu_4NBr in aqueous solvent. Finally, the EM-linker **(2)** was obtained upon treatment of succinic anhydride with compound **1** in presence of Et_3N and catalytic amount of DMAP in $CHCl_3$. Similarly, we synthesized the PODO-linker (**3**) (Fig. 1b) by following the synthesis method of compound **2**. All the synthetic compounds **1**, **2** and **3** were purified over silica gel column chromatography by gradient elution with CH_2Cl_2–MeOH mixture solvent. The structure **1**–**3** were confirmed by ^1H NMR, ^{13}C NMR, and high-resolution mass spectra, and purification was confirmed on RP-HPLC (Fig. S2 and 3). All the synthetic compounds were of 99.9% purity.

In the dendrimer–drug conjugate (D-EM and D-PODO), conjugation was afforded by a typical coupling reaction between hydroxyl-terminated PAMAM dendrimer (D) and linker-drug **2**, **3** in presence of Py-Bop/DIEA in DMF solvent. In this reaction the D was reacted with 18 equivalent of drug-linker **2** and **3** to get the 13 and 12 molecules loading on the dendrimer surface with EM and PODO, respectively. The conjugates were purified by dialysis and identified by analytical RP-HPLC. The chromatogram indicates that there was no low molecular weight starting material impurities. The attachments of linked-drug (**2** and **3**) molecules were indicated by the changes of retention time in RP-HPLC. It was also observed that using 20 or more equivalent of **2** and **3** did not increase the drug loading onto the dendrimer surface. The number of EM and PODO molecules attached to the dendrimer was determined using ^1H NMR (Fig. S4) by comparing the number of the amide and CH_2 protons of dendrimer with the aromatic proton of drugs. The amide protons corresponding to PAMAM appeared between chemical shifts, 7.71–8.08 ppm, while the aromatic D-EM protons appeared as a singlet at 6.81 ppm, but for D-PODO aromatic proton appeared at 6.78 ppm as singlet.

The change of molecular weight was confirmed through MALDI-TOF-MS experiment upon conjugation of the drug molecules to the D-surface. The MALDI-TOF result indicated drug loading to the dendrimer surface were 11 and 10 for the EM and PODO respectively (Fig. S5). It is possible that few free drug molecules may exist in the dimer form in the conjugates. To further confirm loading to the dendrimer surface, we incubated conjugates on 0.1(N) NaOH to release the whole drug and quantify on HPLC against standard graph of EM and PODO. Result indicated the presence of 13 and 12 equivalent molecules of EM and PODO were attached on the dendrimer surface in the conjugates D-EM and D-PODO, respectively. Following incubation of the D-PODO conjugate for 20 min in 0.1 N NaOH, release of all free drugs from conjugates was observed (Fig. S6). However, of all the free PODO were converted to its metabolite 4′-demethylepipodophyllotoxin (DMPODO). But, any such kind of hydrolyzed metabolic product from EM was not detected on HPLC for the D-EM conjugate. As D-EM conjugate contain carbamic ester, hydrolysis need more basic condition and more time [43,44]. The production of DMPODO in this study was determined from the standard curve of the DMPODO. The free drug

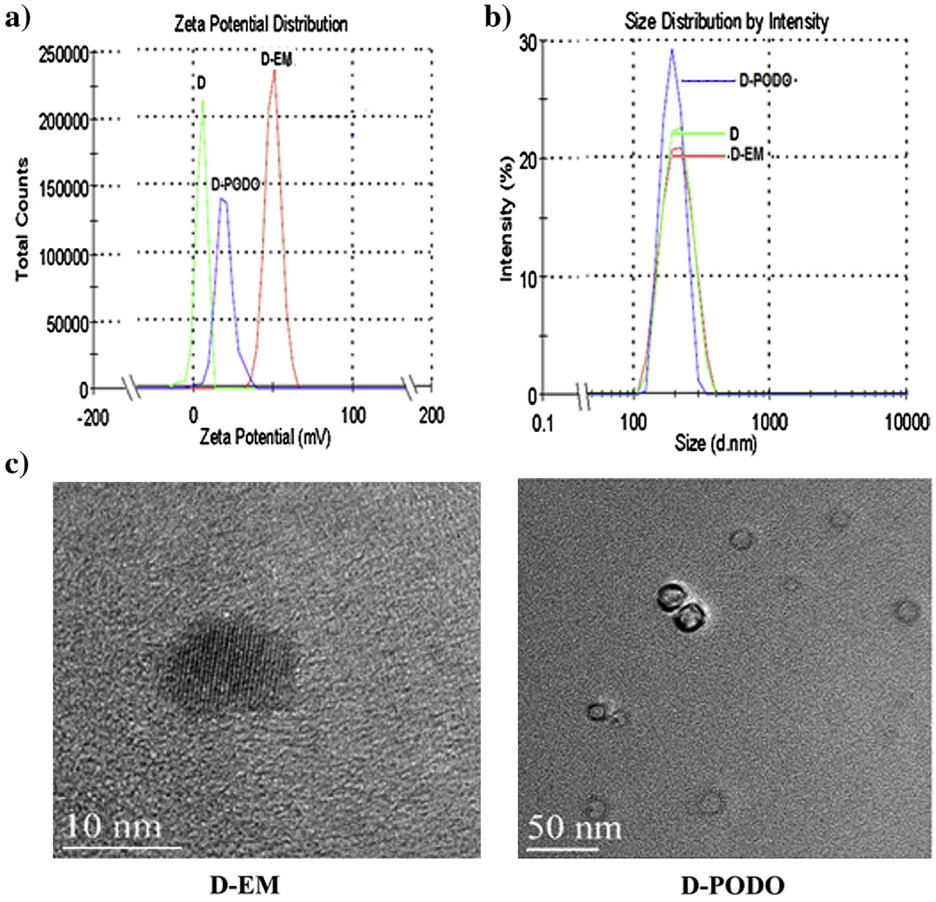

Fig. 2. Zeta potential, DLS and TEM of dendrimer conjugated EM and PODO. (a) Comparative zeta potential of D and dendrimer conjugates D-EM and D-PODO. (b) DLS size measurements of free dendrimer (D) and its conjugates (D-EM and D-PODO). (c) TEM images of dendrimer conjugates. TEM shows D-EM particle size around 10 nm and D-PODO around 8–15 nm.

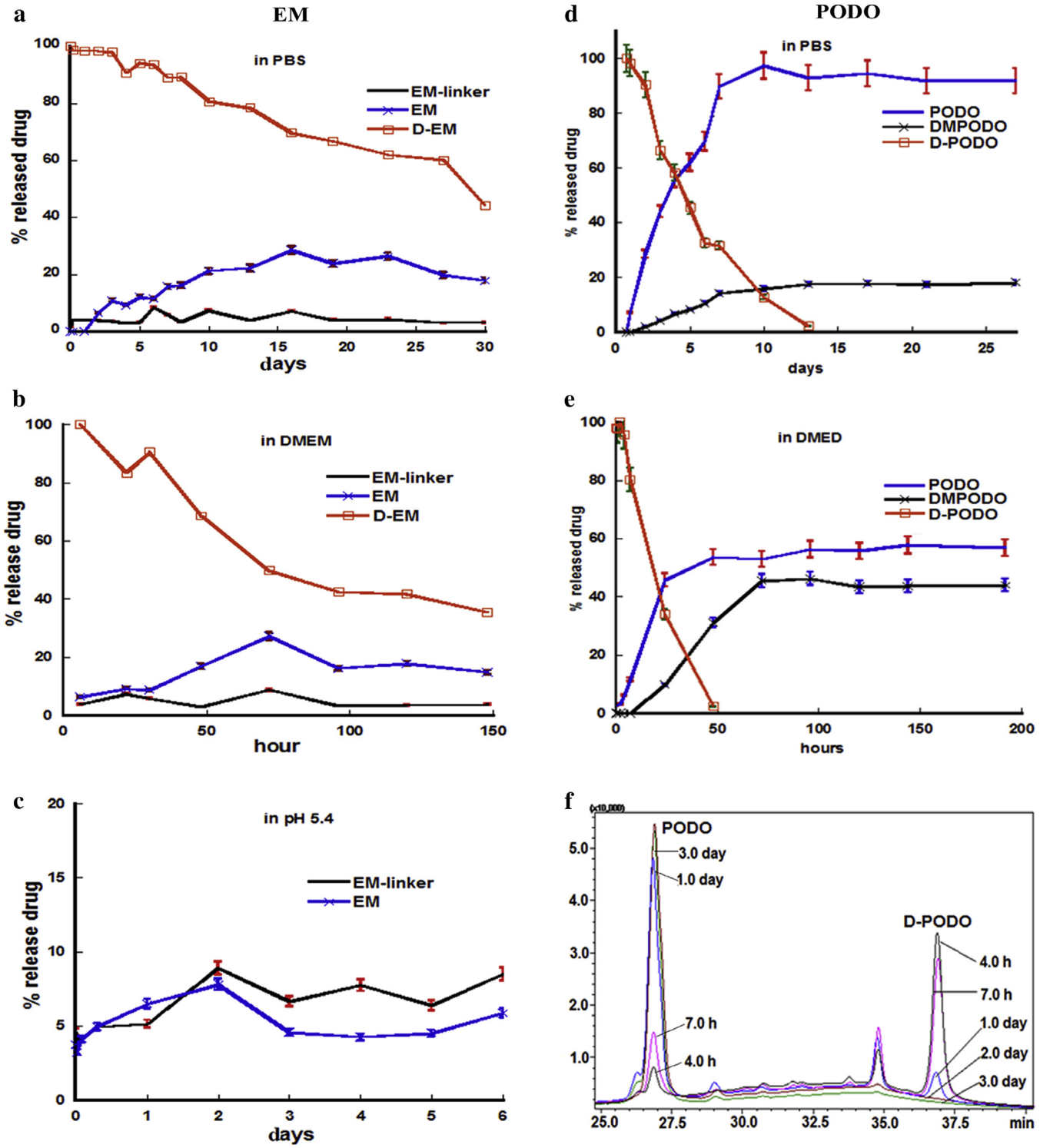

Fig. 3. Controlled release study of free EM and PODO from dendrimer conjugates in PBS, DMEM cell culture medium and acidic pH. Release of EM and EM-linker from D-EM conjugate in 0.1 M PBS buffer and in DMEM medium was monitored by RP-HPLC at 270 nm. D-PODO release study was monitored at 290 nm in RP-HPLC. (a) Decreased concentration of D-EM and increased concentration of EM and EM-linker during 30 days of release profile in PBS (pH 7.4); (b) Release profile of D-EM in DMEM cell culture medium showing decreased concentration of D-EM conjugate and increased concentration of EM and EM-linker during 150 h study; (c) Initial release of the EM from conjugate at pH 5.4; (d) Release study of the free (PODO) from D-PODO conjugate in 0.1 M PBS buffer for 30 days; showing the increase concentration of PODO with time during 25 days and formation of DMPODO(15%) at the end of 25 days. D-PODO conjugates release ~ 95% PODO and DMPODO at the end of 13 days; (e) Release study on DMEM cell culture medium containing 10% FBS showing 55% of the PODO and 40% of the PODO metabolites (DMPODO) released at the end of day 3. The conjugate was nearly zero at the end of day 3; (f) The representative chromatograms of the D-PODO conjugate incubated in DMEM medium at concentration of 2 mg/mL for 4.0 h, 7.0 h, 1 day, 2 day and 3 day, showing increase PODO concentration and decrease concentration of D-PODO.

EM loading on the dendrimer surface was 272 μg/1 mg conjugate whereas D-PODO indicates the loading 259 μg/1 mg conjugate.

3.2. Zeta potential of the conjugates

As most cellular membranes are negatively charged zeta potential can affect a nanoparticle's tendency to permeate membranes, with cationic particles generally showing more toxicity to cell wall disruption [45]. To determine the surface charge of the dendrimer–drug conjugates, we measured their zeta potential in the aqueous solution. The zeta potentials of D (4.64 mV), D-EM (49.6 mV) and D-PODO (19.2 mV) indicated neutral to slightly positive zeta potential (Fig. 2a). These suggest that dendrimer conjugated PODO is more biocompatible and non toxic to the cell membrane, whereas D-EM conjugate showing zeta potential greater than 30 mV could result in greater toxicity to the cell.

3.3. DLS and TEM characterization of the conjugates

The commercially available PAMAM-dendrimer particle size is around 4.5 nm. DLS characterization revealed the hydrodynamic diameter of dendrimer in water to be 228.1 ± 50.32 nm (Fig. 2b) and of D-EM and D-PODO to be 204.7 ± 30.43 nm and 164 ± 20 nm, respectively. The particles sizes of the conjugates were also determined by TEM. Particle size determination by TEM showed both conjugates (D-EM and D-PODO) to be around 8–15 nm (Fig. 2c), of defined shape and to be uniformly distributed.

3.4. Release of the free drugs from conjugates

To understand the stability and the release kinetics of these conjugates, the drug release rates of the conjugates were studied at PBS buffer at physiological pH (7.4). Conjugates D-EM and D-PODO were subjected to hydrolytic cleavage in PBS buffer in a time dependent manner (Fig. 3a and d). The drug release was monitored for 30 days in 0.1 M PBS buffer (pH 7.4). For D-EM conjugate in PBS, the release was slow, with only 10% free drug being released in 48 h. Over 16 days approximately 37% free drugs were released and no further increase of drug release was observed at the end of 30 days period release study. However, comparatively faster release was noted from D-PODO conjugate (Fig. 3d). While initially only 7% free drug was observed within 24 h, greater than 60% drug was released by day 4. By 10 days almost all the free PODO drug was released with D-PODO concentration reaching near zero. The formation of 15% DMPODO (hydrolyzed product from PODO compound) was observed at the end of 30 days study. The formed DMPODO is also reported to have stronger anticancer activity and more soluble than parent drug PODO [46]. The linked drug (PODO-linker) has not been detected on HPLC-chromatogram during release study. The release study indicated that pH 5.4 speeds the initial release of the D-EM conjugate as compared to pH 7.4 (Fig. 3c). The release pattern of D-PODO conjugate was not altered by changes in pH from neutral to acidic. Release of only 10% of free drug release over 6 days (data not shown) indicated that the drug PODO was not tightly holding through inside the cavity of the dendrimer.

The conjugates stability in cell culture media were also monitored to determine whether the potential activity of the conjugates would be due to extracellular and/or intracellular release of the drug [47]. Therefore, the drug released study was monitored in DMEM cell culture medium containing 10% FBS. The release profiles of the conjugates (D-EM and D-PODO) (Fig. 3b and e) were monitored in a time dependent manner for 6 days. The D-EM conjugate release was relatively slow, with only 45% of the free drug EM (including 5% EM-linker) being detected on day 3. There was no initial burst release but drug was released in a sustained manner over the 6 days period. Release study with D-PODO indicated 40% of PODO and 10% of the DMPODO release within 24 h, followed by sustained release. Fig. 3f indicates the enhance peak area of PODO and subsequently decrease peak area for the conjugate D-PODO with increasing time. Almost all the drug was released by 150 h. Inter-conversion of PODO to DMPODO was not observed with time.

3.5. Free and dendrimer conjugates of EM and PODO sensitizes glioma cells to apoptosis

To determine whether the dendrimer conjugates of EM and PODO differ in their ability to affect glioma cell viability as compared to free drugs, glioma cells were treated with EM, PODO, D-EM and D-PODO for 48 h. Treatment with 5 μM of EM resulted in 30, 20 and 10% reduction in viability T98G, A172 and U87MG glioma cell lines, respectively. Though D-EM decreased cell viability further, its ability to affect cell viability was not significantly different from EM. Treatment with 5 μM of D-EM resulted in further 10–14% decrease in viability as compared to EM (Fig. 4a). While treatment with 750 nM PODO resulted in 40, 20 and 10% reduction in viability A172, T98G and U87MG glioma cells respectively, this decrease was further elevated by 12–25% by same concentration of D-PODO (Fig. 4b). D-PODO induced slightly greater reduction in cell viability but the decrease was not statistically significant as compared to free drugs. However, PODO was more effective in inducing cell death as compared to EM.

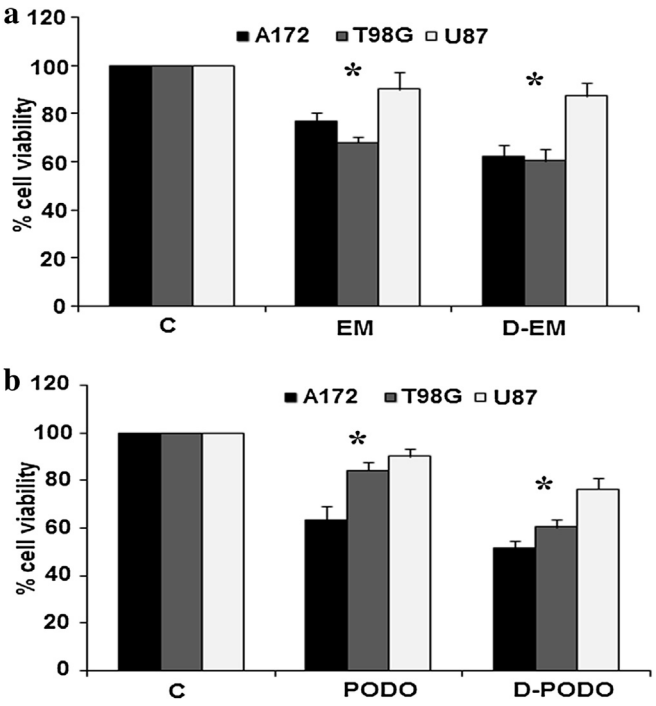

Fig. 4. Free and dendrimer conjugated EM and PODO induces glioma cell death. Viability of glioma cells treated with (a) 5 μM of EM, D-EM (concentration of EM in conjugate) and (b) 750 nM of PODO and D-PODO (concentration of PODO in conjugate), as determined by MTS assay. The graph represents the percentage viable cells of control observed when U87MG, T98G, and A172 cells were treated with free and conjugated drugs for 48 h. Values represent the means ± S.E.M. from three independent experiments. *denotes significant change compared to control ($P < 0.05$).

3.6. Dendrimer conjugates inhibit cell cycle progression effectively than free drugs

As both free drug and dendrimer conjugates decreased cell viability, FACS analysis was performed to determine cell cycle profile in cells treated with EM, PODO, D-EM, and D-PODO (Fig. 5a–d). In T98G cells EM induced G2/M phase arrest (8.36%) as compared to control (5.16%). Treatment with D-EM increased the accumulation of cells at the G2/M phase further (11.56%). EM or D-EM had no effect on % of S phase cells in T98G (Fig. 5a). In U87MG cells, D-EM induced S phase arrest in comparison to control and EM treated cells. A 3.3, 3.4 and 6.4% cells were observed at S phase in control, EM and D-EM treated U87MG cells, respectively. Treatment resulted in 6.7 and 4.2% cells at G2/M phase in EM and D-EM cells,

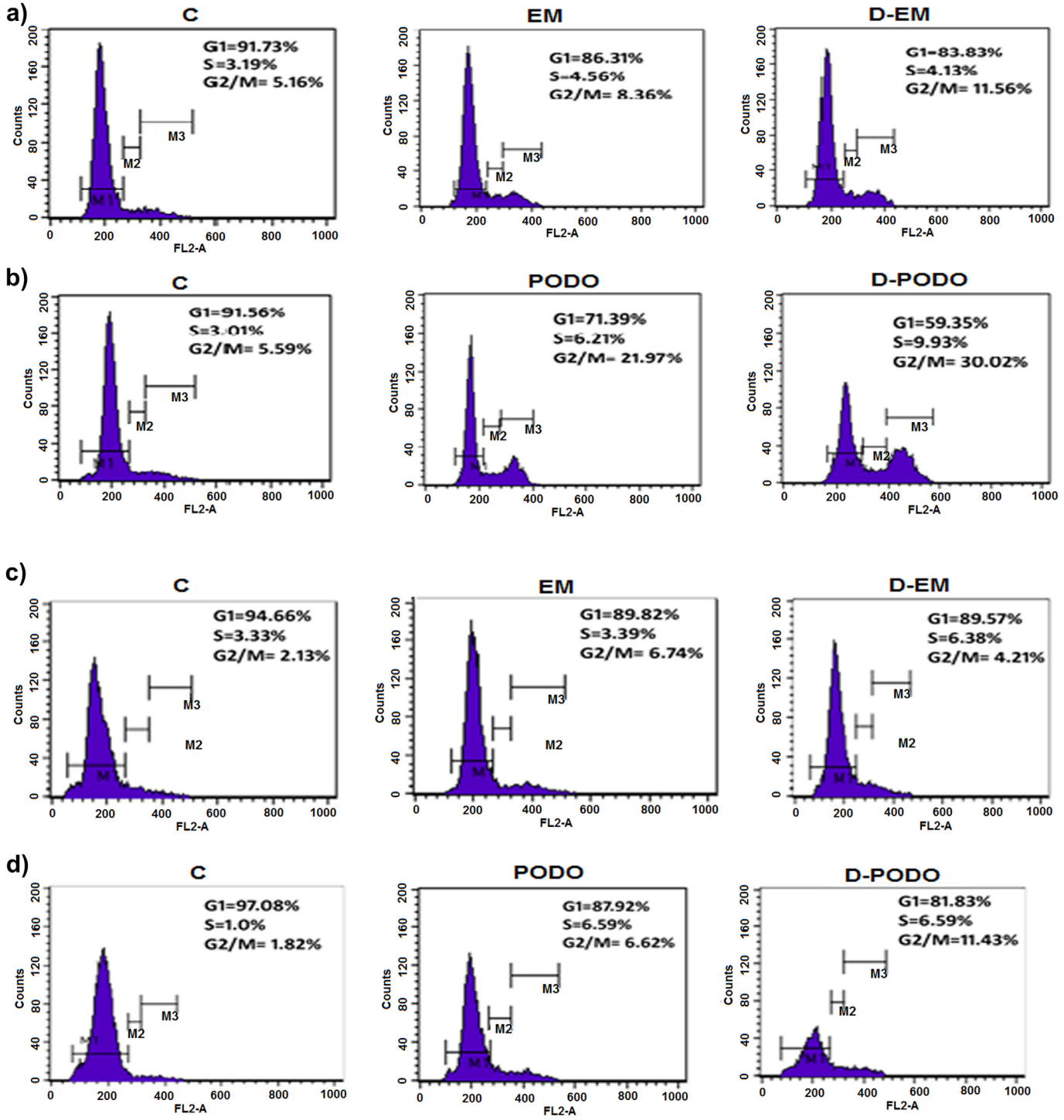

Fig. 5. Dendrimer conjugated EM and PODO affects cell cycle progression effectively than free drugs. FACS analysis was performed on T98G (a and b) and U87MG (c and d) cells treated with EM (5 μM), PODO (750 nM), D-EM (5 μM) and D-PODO (750 nM). An increased % of cells were observed in S and G2/M phase upon treatment with the conjugated drugs. Inset indicates percentage of cells in G1, S and G2/M phase of the cell cycle.

as compared to 2.1% in control (Fig. 5c). In U87MG cells, a 1.8, 6.6, 11.4% cells were observed at G2/M in control, PODO and D-PODO cells, respectively (Fig. 5d). An increase in cell accumulation at S phase was also observed in PODO (6.6%) and D-PODO (6.6%) cells as compared to control (1.0%) (Fig. 5d). Similar trend was observed in T98G cells although the effect on cell cycle arrest by D-PODO was more pronounced (Fig. 5b). An increase in G2/M arrest was observed in T98G cells treated with PODO (21.9%) and D-PODO (30%) as compared to control (5.6%). Free and conjugated PODO also induced arrest in S phase with 3.0, 6.2 and 9.9% cells being observed in control, PODO and D-PODO cells, respectively (Fig. 5b). Cell cycle analysis clearly indicate that D-PODO is efficient at inducing cell cycle arrest as compared to PODO, and at the same time naturally occurring PODO is more effective than synthetic EM.

3.7. Dendrimer conjugated PODO and EM affect tubulin polymerization more effectively than free drug

As the ability of EM and PODO to prevent cell cycle progression is associated with their microtubule inhibitory property, we investigated whether increased cell cycle arrest induced by free and dendrimer conjugated EM and PODO is accompanied by altered tubulin stability. EM and D-EM induced decrease in tubulin polymerization was concomitant with increase in globular fraction, as compared to untreated control (Fig. 6a). The increase in globular fraction was greater in D-EM treated samples than in cells treated with free EM. Similar result was also observed in PODO and D-PODO treated samples (Fig. 6a).

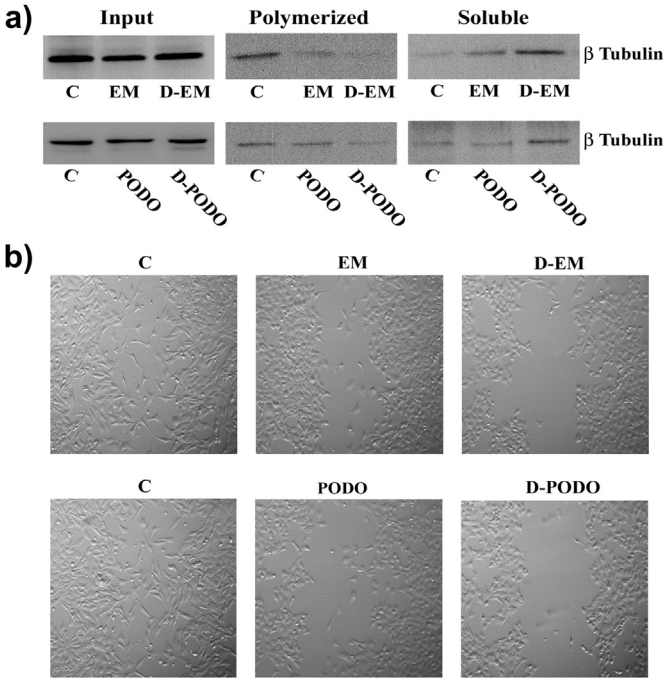

Fig. 6. The ability of-EM and D-PODO to inhibit tubulin polymerization and glioma cell migration is greater than EM and PODO. (a) Representative western blots indicating β tubulin levels in cell lysate and polymerized and soluble microtubule fractions isolated from EM, D-EM, PODO and D-PODO treated T98G glioma cells. Both EM and PODO reduced polymerized β tubulin level. Increased soluble β tubulin levels further confirms the efficacy of the treatment. However, D-EM and D-PODO were more potent in inhibiting microtubule polymerization as compared t**o** EM and PODO respectively. A representative blot is shown from two independent experiments with identical results. (b) Ability of T98G to migrate after scratch wound injury was inhibited more efficiently in the presence of D-EM and D-PODO, as compared to EM and PODO. Micrographs depict cultures of T98G with scratch wound that were left untreated or treated with EM, PODO, D-EM and D-PODO for 24 h. The figure is representative of two independent experiments with similar results.

3.8. Both free and dendrimer conjugated PODO inhibit glioma cell migration more effectively than EM and D-EM

As EM and D-EM are inhibitors of microtubule polymerization which are crucial regulators of cell migration, we investigated the migration ability of glioma cells treated with EM, PODO, D-EM or D-PODO using wound-healing assay (Fig. 6b). There was a decrease in cell migration, as demonstrated by the difference in the wound area covered in EM and PODO treated T98G cells as compared to control. However, the ability of PODO to inhibit migration of cell was greater than EM. Treatment with D-EM and D-PODO reduced migration of glioma cells greatly as compared to free EM and PODO, the efficiency of D-PODO was greater than PODO or D-EM. Thus, the decrease in cell migration as shown by the difference in the wound area covered in EM and PODO treated cells as compared to control, was further enhanced by its dendrimer conjugates D-EM and D-PODO. A similar trend was observed in U87MG and A172 cells (data not shown). Thus, D-PODO is an effective inhibitor of glioma cell motility as compared to its free form or the synthetic EM.

4. Discussion

The dendrimer-based drug delivery has been used broadly for therapeutic drug. Linker or spacer has been used to attach drug molecules to dendrimer surface to enable faster drug release. For this study, we synthesized dendrimer conjugated EM and PODO using succinic acid as linker. Synthetic strategies were aimed to synthesize linker EM and PODO that would possess reactive functional group suitable for efficient conjugation with hydroxy-terminated PAMAM dendrimer (D) in presence of coupling reagents. Our objective was to make an ester linker through hydroxyl group that finally attaches to the dendrimer. The obtained products were pure, of nanometer size, round shaped with improved aqueous solubility as determined by multiple physiochemical analysis (HPLC, NMR, MALDI-TOF, and TEM). The neutral to slightly positive zeta potential surface charges of the dendrimer–drug conjugates is considered good in the context of biological system. Both the drug conjugates were soluble in water. While solubility for EM less than 1 mg/L indicates high improvement of its aqueous solubility [48], the solubility of D-EM conjugate was 20 mg/mL (equivalent to 5.44 mg/mL EM in the conjugate) and D-PODO conjugate was 20 mg/mL (4.92 mg/mL free PODO drug) in water.

Release of the drug from the conjugates is an important part of the drug delivery system. The ester linker from dendrimer–drug conjugates hydrolysis is controlled by pH, and ester bonds are more labile toward hydrolysis as compared with other bond. In our previous report, we have seen only 40% of the drug release at the end of 15 days in PBS buffer which resulted in 4-fold activity against lung epithelial carcinoma cells [39]. In this study, EM is highly hydrophobic in nature and forms strong attraction with the interior part of the dendrimer; as the surface containing electron rich hydroxyl group of the dendrimer shields from hydrolysis of ester bond which is not easily accessible to the nucleophilic water molecules. As a consequence the hydrolytic cleavage of the drug is difficult and the drug release was much slower for D-EM conjugate. The slow release of the EM may be due to the interaction between the drug molecules (hydrophobic EM) and the hydrophobic cavities inside the dendrimer, as well as the drug that remain inside the dendrimer rather than on the surface [49]. However, for conjugate D-PODO it is possible that the bulky, rigid comparatively low lipophilic drug molecule PODO stays on the surface of the dendrimer,

making the ester bond easily accessible (in D-PODO) to nucleophile water molecules and susceptible to hydrolytically cleavage. A low pH increases the initial release of the D-EM conjugates. This may be credited to protonation of tertiary and primary nitrogen groups of dendrimer at low pH and weakening of the hydrophobic interaction of the drug EM with the interior part of the dendrimer, and thereby moving the dendritic-unit outward leaving the cavities wide open and hence enabling release of the drug at a faster rate initially. Similar observations have been previously reported [50].

In this study, FBS containing esterase plays a critical role in cleaving the ester bond between dendrimer and drug and thereby facilitating the release of drug molecules. Esterase can specifically cleave the ester bond between the linker and the drug, whereas in PBS the release is only due to nonspecific hydrolysis. The D-EM conjugate release was relatively slow. There was no initial burst release but drug was released in a sustained manner over the 6 days period. The fact that only ~40% of the free EM is released even after 72 h from conjugates in DMEM cell medium, suggested that the covalent conjugates are quite stable and hold promise as delivery system for controlled release of the drug. Also, EM drug containing nitrogen mustard moiety was un-altered by 10% FBS containing DMEM medium and in PBS, though hydrolysis of the carbamic ester occurs in plasma sample (*in-vitro*) or *in-vivo* human plasma [51,52]. The DMEM medium is not able to cleave the nitrogen mustard moiety in our experimental condition.

Release study with D-PODO indicated 40% of PODO and 10% of the DMPODO release within 24 h, followed by sustained release. The formation of DMPODO (hydrolyzed product from PODO compound) both in PBS and in DMEM was observed with time. DMPODO has been reported to have stronger anticancer activity and more soluble than parent drug PODO [46]. Taken together, release studies in PBS and DMEM indicated stability of both the conjugates against hydrolytic cleavage. Moreover, release of D-EM was found to be comparatively slower than D-PODO. This increase in sustained release of both D-EM and D-PODO could result in subsequent longer circulation time *in-vivo*.

As glioblastoma multiforme, the most malignant of brain tumors, are refractory to conventional chemotherapy we evaluated the efficacy of these conjugates on glioma cell lines *in-vitro*. Treatment of glioma cells with dendrimer conjugates D-EM and D-PODO decreased cell viability, arrested cell cycle progression, inhibited migration and tubulin depolymerization. Interestingly, the effect of the conjugates was greater than the free drug. Thus, conjugation with dendrimer improves the effectiveness of these microtubule inhibitors. As the efficacy of dendrimer conjugated naturally occurring PODO to affect glioma cells in terms of inhibiting proliferation and migration was greater than conjugated synthetic EM, evaluating the importance of D-PODO as potential anti-glioma target warrants investigation.

Acknowledgments

The author Sk UH wish to thank the Director, CSIR-IHBT for providing the necessary facilities; and Dr. B. Singh of NPP Division for his support. Authors also gratefully acknowledge financial assistance from the Department of Science and Technology (Fast track scheme for young scientist), Govt. Of India (Grant No. SR/FT/CS-132/2011, SERB) for awarding fellowship to Sk UH. IHBT COMMUNICATION NUMBER: 3502.

Appendix A. Supplementary data

Supplementary data related to this article can be found at http://dx.doi.org/10.1016/j.ejmech.2013.07.007.

References

[1] G. Jonsson, B. Hogberg, T. Nilsson, Treatment of advanced prostatic carcinoma with estramustine phosphate (Estracyt), Scand. J. Urol. Nephrol. 11 (1977) 231–238.
[2] R. Henriksson, A. Malmstrom, P. Bergstrom, G. Bergh, T. Trojanowski, L. Andreasson, E. Blomquist, S. Jonsborg, T. Edekling, P. Salander, T. Brannstrom, A.T. Bergenheim, High-grade astrocytoma treated concomitantly with estramustine and radiotherapy, J. Neurooncol. 78 (2006) 321–326.
[3] A. Minato, N. Fujimoto, T. Kubo, S. Harada, S. Akasaka, T. Matsumoto, Efficacy of estramustine phosphate according to risk classification of castration-resistant prostate cancer, Med. Oncol. 29 (2012) 2895–2900.
[4] J.M. Piepmeier, D.L. Keefe, M.A. Weinstein, D. Yoshida, J. Zielinski, T.T. Lin, Z. Chen, F. Naftolin, Estramustine and estrone analogs rapidly and reversibly inhibit deoxyribonucleic acid synthesis and alter morphology in cultured human glioblastoma cells, Neurosurgery 32 (1993) 422–430 discussion 430–421.
[5] A.T. Bergenheim, B. Zackrisson, J. Elfverson, G. Roos, R. Henriksson, Radiosensitizing effect of estramustine in malignant glioma in vitro and in vivo, J. Neurooncol 23 (1995) 191–200.
[6] D. Yoshida, S. Hoshino, T. Shimura, H. Takahashi, A. Teramoto, Drug-induced apoptosis by anti-microtubule agent, estramustine phosphate on human malignant glioma cell line, U87MG; in vitro study, J. Neurooncol. 47 (2000) 133–140.
[7] M. Kanje, J. Deinum, M. Wallin, P. Ekstrom, A. Edstrom, B. Hartley-Asp, Effect of estramustine phosphate on the assembly of isolated bovine brain microtubules and fast axonal transport in the frog sciatic nerve, Cancer Res. 45 (1985) 2234–2239.
[8] M.E. Stearns, K.D. Tew, Estramustine binds MAP-2 to inhibit microtubule assembly in vitro, J. Cell Sci. 89 (Pt 3) (1988) 331–342.
[9] R. Benson, B. Hartley-Asp, Mechanisms of action and clinical uses of estramustine, Cancer Invest. 8 (1990) 375–380.
[10] L.C. Marras, W.H. Geerts, J.R. Perry, The risk of venous thromboembolism is increased throughout the course of malignant glioma: an evidence-based review, Cancer 89 (2000) 640–646.
[11] M. Gordaliza, P.A. García, J.M. del Corral, M.A. Castro, M.A. Gómez-Zurita, Podophyllotoxin: distribution, sources, applications and new cytotoxic derivatives, Toxicon 44 (2004) 441–459.
[12] A. Castro, J.M. del Corral, M. Gordaliza, C. Grande, A. Gómez-Zurita, D. García-Grávalos, A. San Feliciano, Synthesis and cytotoxicity of podophyllotoxin analogues modified in the A ring, Eur. J. Med. Chem. 38 (2003) 65–74.
[13] T. Utsugi, J. Shibata, Y. Sugimoto, K. Aoyagi, K. Wierzba, T. Kobunai, T. Terada, T. Oh-hara, T. Tsuruo, Y. Yamada, Antitumor activity of a novel podophyllotoxin derivative (TOP-53) against lung cancer and lung metastatic cancer, Cancer Res. 56 (1996) 2809–2814.
[14] D. Subrahmanyam, B. Renuka, C.V. Rao, P.S. Sagar, D.S. Deevi, J.M. Babu, K. Vyas, Novel D-ring analogues of podophyllotoxin as potent anti-cancer agents, Bioorg. Med. Chem. Lett. 8 (1998) 1391–1396.
[15] R.I. Fisher, E.R. Gaynor, S. Dahlberg, M.M. Oken, T.M. Grogan, E.M. Mize, J.M. Glick, C.A. Coltman Jr., T.P. Miller, A phase III comparison of CHOP vs. m-BACOD vs. ProMACE-CytaBOM vs. MACOP-B in patients with intermediate- or high-grade non-Hodgkin's lymphoma: results of SWOG-8516 (Intergroup 0067), the National High-priority Lymphoma Study, Ann. Oncol. 5 (Suppl. 2) (1994) 91–95.
[16] M. Gordaliza, M.A. Castro, J.M. Miguel del Corral, A. San Feliciano, Antitumor properties of podophyllotoxin and related compounds, Curr. Pharm. Des. 6 (2000) 1811–1839.
[17] H. Xu, M. Lv, X. Tian, A review on hemisynthesis, biosynthesis, biological activities, mode of action, and structure-activity relationship of podophyllotoxins: 2003-2007, Curr. Med. Chem. 16 (2009) 327–349.
[18] M.W. Pettit, P. Griffiths, P. Ferruti, S.C. Richardson, Poly(amidoamine) polymers: soluble linear amphiphilic drug-delivery systems for genes, proteins and oligonucleotides, Ther. Deliv. 2 (2011) 907–917.
[19] W. Qin, K. Yang, H. Tang, L. Tan, Q. Xie, M. Ma, Y. Zhang, S. Yao, Improved GFP gene transfection mediated by polyamidoaminedendrimer-functionalized multi-walled carbon nanotubes with high biocompatibility, Colloids Surf. B Biointerfaces 84 (2011) 206–213.
[20] A.K. Patri, J.F. Kukowska-Latallo, J.R. Baker Jr., Targeted drug delivery with dendrimers: comparison of the release kinetics of covalently conjugated drug and non-covalent drug inclusion complex, Adv. Drug Deliv. Rev. 57 (2005) 2203–2214.
[21] C.C. Lee, J.A. MacKay, J.M. Frechet, F.C. Szoka, Designing dendrimers for biological applications, Nat. Biotechnol. 23 (2005) 1517–1526.
[22] A.R. Menjoge, R.M. Kannan, D.A. Tomalia, Dendrimer-based drug and imaging conjugates: design considerations for nanomedical applications, Drug Discov. Today 15 (2010) 171–185.
[23] S. Svenson, D.A. Tomalia, Dendrimers in biomedical applications–reflections on the field, Adv. Drug Deliv. Rev. 57 (2005) 2106–2129.
[24] J. Khandare, P. Kolhe, O. Pillai, S. Kannan, M. Lieh-Lai, R.M. Kannan, Synthesis, cellular transport, and activity of polyamidoaminedendrimer-methylprednisolone conjugates, Bioconjug. Chem. 16 (2005) 330–337.
[25] J.F. Kukowska-Latallo, K.A. Candido, Z. Cao, S.S. Nigavekar, I.J. Majoros, T.P. Thomas, L.P. Balogh, M.K. Khan, J.R. Baker Jr., Nanoparticle targeting of anticancer drug improves therapeutic response in animal model of human epithelial cancer, Cancer Res. 65 (2005) 5317–5324.

[26] I.J. Majoros, A. Myc, T. Thomas, C.B. Mehta, J.R. Baker Jr., PAMAM dendrimer-based multifunctional conjugate for cancer therapy: synthesis, characterization, and functionality, Biomacromolecules 7 (2006) 572–579.
[27] O.L. Padilla De Jesus, H.R. Ihre, L. Gagne, J.M. Frechet, F.C. Szoka Jr., Polyester dendritic systems for drug delivery applications: in vitro and in vivo evaluation, Bioconjug. Chem. 13 (2002) 453–461.
[28] T.D. McCarthy, P. Karellas, S.A. Henderson, M. Giannis, D.F. O'Keefe, G. Heery, J.R. Paull, B.R. Matthews, G. Holan, Dendrimers as drugs: discovery and preclinical and clinical development of dendrimer-based microbicides for HIV and STI prevention, Mol. Pharm. 2 (2005) 312–318.
[29] X. Shi, I. Lee, X. Chen, M. Shen, S. Xiao, M. Zhu, J.R. Baker, S.H. Wang, Influence of dendrimer surface charge on the bioactivity of 2-methoxyestradiol complexed with dendrimers, Soft Matter 6 (2010) 2539–2545.
[30] S. Kannan, H. Dai, R.S. Navath, B. Balakrishnan, A. Jyoti, J. Janisse, R. Romero, R.M. Kannan, Dendrimer-based postnatal therapy for neuroinflammation and cerebral palsy in a rabbit model, Sci. Transl. Med. 4 (2012) 130–146.
[31] B. Wang, R.S. Navath, A.R. Menjoge, B. Balakrishnan, R. Bellair, H. Dai, R. Romero, S. Kannan, R.M. Kannan, Inhibition of bacterial growth and intramniotic infection in a guinea pig model of chorioamnionitis using PAMAM dendrimers, Int. J. Pharm. 395 (2010) 298–308.
[32] C. Kang, X. Yuan, F. Li, P. Pu, S. Yu, C. Shen, Z. Zhang, Y. Zhang, Evaluation of folate-PAMAM for the delivery of antisense oligonucleotides to rat C6 glioma cells in vitro and in vivo, J. Biomed. Mater. Res. A 93 (2010) 585–594.
[33] Y. Li, H. He, X. Jia, W.L. Lu, J. Lou, Y. Wei, A dual-targeting nanocarrier based on poly(amidoamine) dendrimers conjugated with transferrin and tamoxifen for treating brain gliomas, Biomaterials 33 (2012) 3899–3908.
[34] N. Sakaguchi, C. Kojima, A. Harada, K. Koiwai, K. Kono, The correlation between fusion capability and transfection activity in hybrid complexes of lipoplexes and pH-sensitive liposomes, Biomaterials 29 (2008) 4029–4036.
[35] C. Kojima, T. Suehiro, K. Watanabe, M. Ogawa, A. Fukuhara, E. Nishisaka, A. Harada, K. Kono, T. Inui, Y. Magata, Doxorubicin-conjugated dendrimer/collagen hybrid gels for metastasis-associated drug delivery systems, Acta Biomater. 9 (2013) 5673–5680.
[36] Y.H. Choe, C.D. Conover, D. Wu, M. Royzen, R.B. Greenwald, Anticancer drug delivery systems: N4-acyl poly(ethyleneglycol) prodrugs of ara-C. I. Efficacy in solid tumors, J. Control. Release 79 (2002) 41–53.
[37] R. Duncan, Drug-polymer conjugates: potential for improved chemotherapy, Anticancer Drugs 3 (1992) 175–210.
[38] R.B. Greenwald, C.D. Conover, A. Pendri, Y.H. Choe, A. Martinez, D. Wu, S. Guan, Z. Yao, K.L. Shum, Drug delivery of anticancer agents: water soluble 4-poly (ethylene glycol) derivatives of the lignan, podophyllotoxin, J. Control Release 61 (1999) 281–294.
[39] U.H. Sk, S.P. Kambhampati, M.K. Mishra, W.G. Lesniak, F. Zhang, R.M. Kannan, Enhancing the efficacy of Ara-C through conjugation with PAMAM dendrimer and linear PEG: a comparative study, Biomacromolecules 14 (2013) 801–810.
[40] N. Koul, V. Sharma, D. Dixit, S. Ghosh, E. Sen, Bicyclic triterpenoid iripallidal induces apoptosis and inhibits Akt/mTOR pathway in glioma cells, BMC Cancer 10 (2010) 328.
[41] D. Dixit, V. Sharma, S. Ghosh, V.S. Mehta, E. Sen, Inhibition of casein kinase-2 induces p53-dependent cell cycle arrest and sensitizes glioblastoma cells to tumor necrosis factor (TNFalpha)-induced apoptosis through SIRT1 inhibition, Cell Death Dis. 3 (2011) e271.
[42] R. Tewari, V. Sharma, N. Koul, A. Ghosh, C. Joseph, U.H. Sk, E. Sen, Ebselen abrogates TNFalpha induced pro-inflammatory response in glioblastoma, Mol. Oncol. 3 (2009) 77–83.
[43] E. Humeres, M.N. Sanchez, C.M. L Lobato, N.A. Debacher, E.P. Souza, The mechanisms of hydrolysis of alkyl N-alkylthioncarbamate esters at 100 °C, Can. J. Chem. 83 (2005) 1483–1491.
[44] J. Savolainen, J. Leppanen, M. Forsberg, H. Taipale, T. Nevalainen, J. Huuskonen, J. Gynther, P.T. Mannisto, T. Jarvinen, Synthesis and in vitro/in vivo evaluation of novel oral N-alkyl- and N, N-dialkyl-carbamate esters of entacapone, Life Sci. 67 (2000) 205–216.
[45] J.D. Clogston, A.K. Patri, Zeta potential measurement. Zeta potential measurement, Methods Mol. Biol. 697 (2011) 63–70.
[46] Z. Xiao, K.F. Bastow, J.R. Vance, K.H. Lee, Antitumor agents. Part 227: studies on novel 4′-O-demethyl-epipodophyllotoxins as antitumor agents targeting topoisomerase II, Bioorg. Med. Chem. 12 (2004) 3339–3344.
[47] N. Vijayalakshmi, A. Ray, A. Malugin, H. Ghandehari, Carboxyl-terminated PAMAM-SN38 conjugates: synthesis, characterization, and in vitro evaluation, Bioconjug. Chem. 21 (2010) 1804–1810.
[48] T. Wadsten, N.O. Lindberg, Polymorphism of estramustine, Pharm. Sci. 78 (1989) 563–566.
[49] A. Agarwal, U. Gupta, A. Asthana, N.K. Jain, Dextran conjugated dendritic nanoconstructs as potential vectors for anti-cancer agent, Biomaterials 30 (2009) 3588–3596.
[50] N.K. Jain, U. Gupta, Application of dendrimer-drug complexation in the enhancement of drug solubility and bioavailability, Expert Opin. Drug Metab.Toxicol. 4 (2008) 1035–1052.
[51] B.J. Norlén, S.B. Andersson, P. Björk, P.O. Gunnarsson, A. Fritjofsson, Uptake of estramustine phosphate (estracyt) metabolites in prostatic cancer, J. Urol. 140 (1988) 1058–1062.
[52] O. Gunnarsson, S.B. Andersson, S.A. Johansson, The hydrolysis of estramustine phosphate; in vitro studies, Eur. J. Drug Metab. Pharmacokinet. 8 (1983) 395–402.